Comparative Analysis of Cone and Rod Transducins Using Chimeric Gα Subunits

ARTICLE *in* BIOCHEMISTRY · FEBRUARY 2012

Impact Factor: 3.02 · DOI: 10.1021/bi3000935 · Source: PubMed

3 AUTHORS, INCLUDING:

Kota Gopalakrishna
University of Iowa
15 PUBLICATIONS **121** CITATIONS
SEE PROFILE

Kimberly K Boyd
University of Iowa
15 PUBLICATIONS **204** CITATIONS
SEE PROFILE

Published in final edited form as:
Biochemistry. 2012 February 28; 51(8): 1617–1624. doi:10.1021/bi3000935.

Comparative analysis of cone and rod transducins using chimeric Gα-subunits†

Kota N. Gopalakrishna[1], **Kimberly K. Boyd**[1], and **Nikolai O. Artemyev**[1,2,*]

[1]Department of Molecular Physiology and Biophysics, University of Iowa Carver College of Medicine, Iowa City, IA 52242

[2]Department of Ophthalmology and Visual Sciences, University of Iowa Carver College of Medicine, Iowa City, IA 52242

Abstract

The molecular nature of transducin-α subunits ($G\alpha_t$) may contribute to the distinct physiology of cone and rod photoreceptors. Biochemical properties of mammalian cone $G\alpha_{t2}$-subunits and their differences with rod $G\alpha_{t1}$ are largely unknown. Here, we examined properties of chimeric $G\alpha_{t2}$ in comparison with its rod counterpart. The key biochemical difference between the rod- and cone-like $G\alpha_t$ was ~10-fold higher intrinsic nucleotide exchange on the chimeric $G\alpha_{t2}$. Presented mutational analysis suggests that weaker interdomain interactions between the GTPase (Ras-like) domain and the helical domain in $G\alpha_{t2}$ are in part responsible for its increased spontaneous nucleotide exchange. However, the rates of R*-dependent nucleotide exchange of chimeric $G\alpha_{t2}$ and $G\alpha_{t1}$ were equivalent. Furthermore, chimeric $G\alpha_{t2}$ and $G\alpha_{t1}$ exhibited similar rates of intrinsic GTPase activity as well as similar acceleration of GTP hydrolysis by the RGS domain of RGS9. Our results suggest that the activation and inactivation properties of cone and rod $G\alpha_t$–subunits in an *in vitro* reconstituted system are comparable.

The two types of photoreceptors in the vertebrate retina, rods and cones, mediate vision at dim and bright light, respectively. Cones produce small rapidly-decaying responses and are much less sensitive to light than rods. The molecular basis for the differences in physiology of rods and cones are poorly understood. The phototransduction cascades in rods and cones utilize homologous components including visual pigments, heterotrimeric G proteins (transducins), and cGMP-phosphodiesterases (PDE6) (1–3). In rods, a robust amplification in the signaling cascade is achieved due to a high rate of transducin activation by photolyzed rhodopsin (Meta II or R*) and rapid hydrolysis of cGMP by transducin-activated PDE6. Consistent with the low sensitivity of cones, the signal amplification in mouse cone phototransduction was found to be lower (4). The molecular differences between major cone and rod signaling proteins have been examined as a probable origin of the physiological differences (5–9). Current evidence does not implicate the signaling properties of rod and cone visual pigments. Expression of rhodopsin and red cone pigment in *Xenopus* cones and rods, respectively, yielded responses identical to those of native *Xenopus* photoreceptors (5). Recent physiological analysis points to an important role of transducin α-subunits in shaping specific photoresponses (7). Rods of *GNAT2C* transgenic mice with substitution of rod $G\alpha_{t1}$

†This work was supported by National Institutes of Health Grant EY-12682.

*To whom correspondence should be addressed: Tel.: 319-335-7864; Fax: 319-335-7330; nikolai-artemyev@uiowa.edu.

Supporting Information available

Figure S1 shows sequence alignment of $G\alpha_{t1}$, $G\alpha_{t2}$, $G\alpha_{i1}$, and chimeric $G\alpha_{t1}'$and $G\alpha_{t2}'$. Figure S2 shows the kinetics of GTPγS binding to $G\alpha_{t1}'$ and $G\alpha_{t2}'$ under the conditions of the single-turnover GTPase assay. Figure S3 shows GTPase activity of $G\alpha_{t2}'$-2 in the single-turnover assay. Supplemental materials may be accessed free of charge online at http://pubs.acs.org.

for cone $G\alpha_{t2}$ displayed decreased sensitivity, reduced rate of activation, and accelerated recovery characteristic of cone photoreceptors (7). Reduced rate of cascade activation may result from a slower rate of R*-dependent activation of the $G\alpha_{t2}$ complex with rod-specific $G\beta_1\gamma_1$ or less efficient activation of PDE6 by $G\alpha_{t2}$ (10). Accelerated recovery of *GNAT2C* rods suggests faster GTP hydrolysis in the transition complex of $G\alpha_{t2}$ with PDE6 and the RGS9-1 GTPase accelerating protein (GAP) complex (11). Thus, $G\alpha_{t2}$ may have a higher intrinsic rate of GTP hydrolysis and/or a greater GTPase potentiation by the GAP complex than $G\alpha_{t1}$.

In contrast to well-characterized rod $G\alpha_{t1}$, biochemical properties of $G\alpha_{t2}$ have not been investigated. Native $G\alpha_{t1}$ is readily available for biochemical analyses, whereas the sparsity of cones in mammalian retina impedes isolation of native $G\alpha_{t2}$. In addition, a wealth of information about $G\alpha_{t1}$ properties, including its interaction with R*, PDE6 and RGS9, was developed using robust bacterial expression of transducin-like $G\alpha_{t1}/G\alpha_{i1}$ chimeras (12–14). Here, we applied a chimera approach to analyze key signaling properties of $G\alpha_{t2}$. A $G\alpha_{t2}/G\alpha_{i1}$ chimera ($G\alpha_{t2}'$) was produced and investigated in comparison to analogous $G\alpha_{t1}/G\alpha_{i1}$ chimera Chi8 (13), termed hereafter $G\alpha_{t1}'$. $G\alpha_{t2}'$ and $G\alpha_{t1}'$ are ~94% identical to $G\alpha_{t2}$ and $G\alpha_{t1}$, respectively, which is significantly greater than the degree of homology between $G\alpha_{t2}$ and $G\alpha_{t1}$ (~82%). $G\alpha_{t2}'$ showed a large ~10-fold increase in spontaneous nucleotide exchange rate in comparison to $G\alpha_{t1}'$. A series of chimeric and mutant $G\alpha_t$ subunits delineated $G\alpha_{t2}'$ residues responsible for high intrinsic nucleotide exchange rate. In contrast, the rates of R*-dependent nucleotide exchange were comparable for $G\alpha_{t2}'$ and $G\alpha_{t1}'$ reconstituted with $G\beta_1\gamma_1$. Furthermore, $G\alpha_{t2}'$ and $G\alpha_{t1}'$ exhibited similar rates of intrinsic GTPase activity as well as similar acceleration of GTP hydrolysis by RGS9.

Experimental procedures

Materials

Guanosine 5′-[γ-^{35}S]thiotriphosphate triethylammonium salt (GTPγS; 1100 Ci/mmol), guanosine 5′-[γ-^{32}P]triphosphate triethylammonium salt (~5000Ci/mmol), and nicotinamide adenine dinucleotide ([^{32}P]NAD; 800 Ci/mmol) were from PerkinElmer. Pertussis toxin was from Sigma. Bovine outer rod segment (ROS) membranes were prepared as described (15). Urea-washed ROS membranes (uROS) were prepared according to a published protocol (16). Recombinant $G\beta_1\gamma_1$ complex was expressed using the baculovirus/sf9 cell system and isolated as described (17). The RGS-domain of RGS9 (RGS9d, aa 284–461) was expressed and purified as previously described (14).

Cloning, experession and purification of chimeric $G\alpha_t$ subunits

To obtain chimera $G\alpha_{t2}'$-2 (Fig. 1), the full-length $G\alpha_{t1}'$ (Chi8) sequence was PCR-amplified from the plasmid (13) with a pair of sequence-specific primers (reverse primer contained BamHI site) and cut with BamHI to isolate a 430-bp fragment coding the C-terminal portion of $G\alpha_{t1}'$. This fragment was inserted into the large fragment of the pET15b-$G\alpha_{t2}$ vector (9) digested with BamHI, thereby replacing the C-terminal portion of $G\alpha_{t2}$ with the corresponding fragment of $G\alpha_{t1}'$. Correct orientation of the insert was selected by sequencing the construct. $G\alpha_{t2}'$ was generated from $G\alpha_{t2}'$-2 by replacing three $G\alpha_{t1}$-specific residues, Val301, Glu305 and Arg310, with the corresponding $G\alpha_{t2}$-specific residues Ser305, Asp309, and Lys314. The triple mutant was produced using the QuikChange mutagenesis protocol (Stratagene). The same mutagenesis procedure was used to generate the A144S mutant of $G\alpha_{t2}'$and the following single, double, and triple mutants of $G\alpha_{t1}'$: S140A, K117P/S120V, S153N/D154Q, and V159T/T160D/G162E.

Chimeras $G\alpha_{t2}'$-3 and $G\alpha_{t2}'$-4 were produced by swapping the residues 1–116 and 117–215 of $G\alpha_{t1}'$ with residues 1–120 and 121–219 of $G\alpha_{t2}$, respectively. The $G\alpha_{t2}'$-1-120 sequence was amplified from the $G\alpha_{t2}'$-template using a 5′-primer containing an NcoI site and a 3′-primer with a flanking $G\alpha_{t1}'$ sequence. The resulting PC product was paired with a 3′ primer containing a HindIII site in PC amplification from the $G\alpha_{t1}'$ template to produce the $G\alpha_{t2}'$-3 sequence, which was then cloned into the NcoI/HindIII sites of the pHis6 vector (13). To produce $G\alpha_{t2}'$-4, the $G\alpha_{t1}'$-1-116 sequence was amplified from the $G\alpha_{t1}'$ template using a 5′-primer containing an NcoI site and a 3′-primer with a flanking $G\alpha_{t2}'$ sequence. The resulting PC product was paired with a 3′ primer containing a XhoI site in PC amplification from the $G\alpha_{t2}'$-2 template to produce the $G\alpha_{t2}'$-4 sequence, which was then cloned into the NcoI/XhoI sites of the pET15b vector. Upon sequence verification, protein expression of $G\alpha_{t1}'$, $G\alpha_{t2}'$, their derivatives and mutants, was induced in BL21(DE3) codonPlus competent cells with 30 μM IPTG at 16°C overnight. His_6-tagged proteins were purified on His-bind Ni-NTA resin (Novagen) followed by an ion-exchange chromatography on Uno-Q1 column (Bio-Rad). Fractions containing functional Gα-subunits were dialyzed against buffer containing 40% glycerol overnight and stored at −20°C.

GTPγS binding assay

Chimeric $G\alpha_t$ subunits (1 μM) alone, or mixed with 1 μM $G\beta_1\gamma_1$ and uROS membranes (0.25, 1 or 2 μM rhodopsin), were incubated for 2 min at 25ºC in the presence of light. Binding reactions were started with the addition of 5 μM or 100 nM [^{35}S]GTPγS. Aliquots of 15 μl were withdrawn at the indicated times, mixed with 1 ml ice-cold 20 mM Tris-HCl (pH 8.0) buffer containing 130 mM NaCl, 2 mM $MgSO_4$, and 1 mM GTP, passed through Whatman cellulose nitrate filters (0.45 μm), and washed three times with 3 ml of the same buffer without GTP. The filters were dissolved in 5 ml of a xylene-based 3a70B counting cocktail (RPI Corp.) and [^{35}S]GTPγS was measured in a liquid scintillation counter (18). The k_{app} values for the binding reactions were calculated by fitting data with equation %GTPγS bound=$100(1\text{-}e^{-kt})$. Groups of measurements were compared with two-tailed unpaired *t* test.

GTPase activity assays

Single-turnover GTPase activity measurements were carried out in suspensions of uROS membranes (10 μM rhodopsin) reconstituted with chimeric $G\alpha_t$ subunits (1 μM) and $G\beta_1\gamma_1$ (1 μM) in 10 mM Tris-HCl (pH 7.5) buffer containing 100 mM NaCl and 4 mM $MgSO_4$ (18, 19). Where indicated, RGS9d (3 or 6 μM) was added. After incubation for 5 min at 25ºC, 100 nM [γ-^{32}P]GTP was added to the mixtures to initiate the reaction. GTPase hydrolysis was quenched at the indicated times by mixing 10 μl aliquots with 100 μl of 6 % (v/v) perchloric acid. Nucleotides were precipitated with 700 μl of 10% (w/v) charcoal suspension in phosphate-buffered saline, and free [$^{32}P_i$] was measured by liquid scintillation counting. GTPase rate constants were calculated by fitting the data equation %GTP hydrolyzed = $100(1\text{-}e^{-kt})$, where k_{cat} is the rate constant for GTP hydrolysis.

Pertussis toxin-catalyzed ADP-ribosylation

Chimeric $G\alpha_t$ subunits (0.5 μM each) were mixed with $G\beta_1\gamma_1$ (0.5–2 μM) in 50 μl of 20 mM Tris-HCl (pH 8.0) buffer containing 2 mM $MgSO_4$, 2 mM dithiothreitol, 1 mM EDTA, 10 μM GDP and 5 μg/ml pertussis toxin (preactivated with 100 mM dithiothreitol and 0.25%SDS for 10 min at 30°C). The reaction was started by addition of 5 μM [^{32}P]NAD and allowed to proceed for 1 hr at 25°C. Reaction mixtures were diluted with 1 ml of ice-cold 20 mM Tris-HCl (pH 8.0) buffer containing 100 mM NaCl and filtered through Whatman cellulose-nitrate filters. The filters were washed four times with the same buffer and counted in a liquid scintillation counter. Aliquots (10 μl) were withdrawn from reaction mixtures,

mixed with sample buffer for SDS-PAGE and analyzed by SDS-PAGE and autoradiography.

Results

Increased spontaneous nucleotide exchange in chimeric $G\alpha_{t2}$ subunits

To examine the biochemical properties of cone transducin-α, we generated a chimeric $G\alpha_{t2}'$-subunit, which is a counterpart of previously characterized $G\alpha_{t1}/G\alpha_{i1}$ chimera Chi8 or $G\alpha_{t1}'$ (13) (Fig. 1A). This choice of a chimeric template is based on the efficient bacterial expression of $G\alpha_{t1}'$ and the fact that it is 94% identical to $G\alpha_{t1}$ and appears to recapitulate its essential signaling characteristics. Indeed, expression of functional $G\alpha_{t2}'$ in *E. coli* was similarly robust, and the protein is readily purified (Fig. 1B).

In comparison to $G\alpha_{i1}$, native $G\alpha_{t1}$ and $G\alpha_{t1}/G\alpha_{i1}$ chimeras containing 215 N-terminal residues of $G\alpha_{t1}$ have been shown to have very slow rates of spontaneous guanine nucleotide exchange rate (13). In agreement, the basal rate of GTPγS-binding to $G\alpha_{t1}'$ under our experimental conditions was 0.0050±0.0006 min^{-1}. In contrast to $G\alpha_{t1}'$, $G\alpha_{t2}'$ showed markedly higher intrinsic GTPγS-binding rate (0.048±0.003 min^{-1}) (Fig. 2). Next, we tested chimeric $G\alpha_{t2}'$-2, containing 219 N-terminal residues of $G\alpha_{t2}$ (Fig. 1A). The basal GTPγS-binding rate for $G\alpha_{t2}'$-2 was similar to that of $G\alpha_{t2}'$ (Fig. 2), suggesting that the N-terminal part of $G\alpha_{t2}'$ is responsible for the increased nucleotide exchange. Chimeras $G\alpha_{t2}'$-3 and $G\alpha_{t2}'$-4 were produced by swapping the residues 1–116 and 117–215 of $G\alpha_{t1}'$ with the corresponding residues of $G\alpha_{t2}$ (Fig. 1A). The rate of GTPγS binding to $G\alpha_{t2}'$-4 was nearly as high as that for $G\alpha_{t2}'$, whereas $G\alpha_{t2}'$-3 demonstrated relatively small ~1.7-fold increase in the binding rate over $G\alpha_{t1}'$ (p=0.016) (Fig. 2). The $G\alpha_t$ determinants of the spontaneous nucleotide exchange within the $G\alpha_{t1}$(117–215) region were further probed by mutational analysis of $G\alpha_{t1}'$. This region contains only a few residues that are different between rod and cone $G\alpha_t$, but strongly conserved within each transducin family (Suppl. Fig 1). The following single, double, and triple mutations replacing rod-specific residues with their cone-specific counterparts were introduced into $G\alpha_{t1}'$: S140A, K117P/S120V, S153N/D154Q, and V159T/T160D/G162E (Fig. 3A). The double and triple mutations did not significantly alter the GTPγS-binding rate of $G\alpha_{t1}'$, while the S140A substitution led to a moderate 1.8-fold increase in the k_{app} value for GTPγS binding (p=0.001) (Fig. 3B). We then examined if the reverse mutation A144S in $G\alpha_{t2}'$ would alter its nucleotide exchange kinetics (Fig 3C,D). Indeed, the GTPγS-binding rate of the A144S mutant was 1.7-fold lower than that of $G\alpha_{t2}'$(p=0.004) (Fig. 3D).

Binding of GTPγS to Gα subunits with high spontaneous nucleotide exchange such as $G\alpha_i'$ or $G\alpha_s'$ can often be inhibited by Gβγ-subunits (20, 21). $G\beta_1\gamma_1$ had no effect on the basal rate of GTPγS binding to $G\alpha_{t2}'$ (Fig. 3E).

Pertussis toxin-catalyzed ADP-ribosylation

Binding of $G\beta_1\gamma_1$-subunits to $G\alpha_{t1}$ facilitates pertussis toxin-catalyzed ADP-ribosylation at Cys347 of $G\alpha_{t1}$ (22–24). We utilized this reaction to assess the interactions of $G\alpha_{t1}'$ and $G\alpha_{t2}'$with $G\beta_1\gamma_1$. Pertussis toxin-catalyzed ADP-ribosylation of $G\alpha_{t1}'$ and $G\alpha_{t2}'$ were carried out in the absence or presence of increasing concentrations of $G\beta_1\gamma_1$. The basal level of ADP-ribosylation in the absence of $G\beta_1\gamma_1$ was somewhat higher for $G\alpha_{t2}'$ compared to $G\alpha_{t1}'$ (Fig. 4). The dose-dependencies of $G\beta_1\gamma_1$-supported ADP-ribosylation were comparable for $G\alpha_{t1}'$ and $G\alpha_{t2}'$ suggesting similar submicromolar K_d values for $G\beta_1\gamma_1$ binding (Fig. 4).

Rhodopsin-catalyzed activation of chimeric $G\alpha_{t2}$ and $G\alpha_{t1}$ reconstituted with $G\beta_1\gamma_1$

The efficiencies of activation of $G\alpha_{t2}'$ and $G\alpha_{t1}'$ by R* were measured using a GTPγS-binding assay and reconstitution of the Gα-subunits with $G\beta_1\gamma_1$ and uROS. Suspensions of uROS containing 0.25 μM and 1 μM R* were used to ensure that the GTPγS-binding rates are submaximal. In the presence of uROS containing 0.25 μM R*, the rates of R*-dependent GTPγS binding to $G\alpha_{t2}'$ (k_{app} 0.0045±0.0005 s^{-1} or 0.27 min^{-1}) and $G\alpha_{t1}'$(k_{app} 0.0048±0.0008 s^{-1} or 0.29 min^{-1}) were similar and much greater than the unstimulated rates (Fig. 5). In the presence of uROS containing 1 μM R*, the GTPγS-binding rates to $G\alpha_{t2}'$ and $G\alpha_{t1}'$ were higher still (~0.011 s^{-1} or 0.7 min^{-1}) (Fig. 5). No significant differences were seen in the activation kinetics of the two $G\alpha_t$ proteins.

GTPase activity of chimeric $G\alpha_{t2}$ and $G\alpha_{t1}$ and the effects of RGS9d

The catalytic rates of GTP hydrolysis for $G\alpha_{t2}'$ and $G\alpha_{t2}'$-2 were determined in comparison to $G\alpha_{t1}'$ using a single turnover assay (GTP=100 nM ≪ $G\alpha_t\beta_1\gamma_1$=1 μM) and a high concentration of uROS (10 μM R*). Using uROS containing 2 μM R* and 100 nM GTPγS, the rates of GTPγS-binding to $G\alpha_{t1}'$ and $G\alpha_{t2}'$ were significantly faster than the measured rates of GTP hydrolysis (Suppl. Fig. 2). Thus, the guanine nucleotide binding rates did not limit GTPase reactions under our experimental conditions. The intrinsic GTPase activity of $G\alpha_{t2}'$ (k=0.024±0.001 s^{-1}) was not significantly different from that of $G\alpha_{t1}'$ (k=0.023±0.001 s^{-1}) (Fig. 6). The rate of GTP hydrolysis by $G\alpha_{t2}'$-2 was also similar to that of $G\alpha_{t1}'$ (Suppl. Fig. 3).

The ability of the RGS9-284-461 domain to stimulate GTPase activity of $G\alpha_{t2}'$ and $G\alpha_{t1}'$ was measured at two RGS-protein concentrations, 3 and 6 μM. RGS9-284-461 comparably stimulated GTPase activities of the cone and rod chimeric Gα-subunits. The levels of GTPase activity of $G\alpha_{t2}'$ and $G\alpha_{t1}'$ were ~ 2.2–2.5 and ~3-fold higher in the presence of 3 μM and 6 μM RGS9-284–461, respectively (Fig. 6B).

Discussion

The role of transducin-α subunit in setting the sensitivity and kinetics of light responses of rods and cones has been actively debated (6, 7, 25). Electrophysiological recordings from mouse cones indicate that in mouse S- and M-cones the amplification of phototransduction is 2–3 fold lower and the inactivation is considerably faster than in rods (4). In view of the similar catalytic efficiencies of rod and cone PDE6 (9) and the smaller size of cone outer segment, the lower amplification implies at least 5-fold lower rate of PDE6 activation per activated pigment molecule in mouse cones compared to rods (4). Replacing the rod $G\alpha_{t1}$ with the cone $G\alpha_{t2}$ reduced the amplification in mouse rods by ~2-fold, and speeded up the recovery phase by ~2 – fold, suggesting that the differences in the rod and cone responses might be attributed to a significant extent to the nature of $G\alpha_t$ (7). We sought to determine the biochemical basis underlying the physiological changes induced by $G\alpha_{t2}$ in *GNAT2C* rods. Although, the functional GTPγS-bound form of $G\alpha_{t2}$ can be isolated following transducin expression in *E. coli* (9), this preparation cannot be used to study the activation of Gt by R* or $G\alpha_{t2}$ GTPase activity. Therefore, we produced and examined chimeric $G\alpha_{t2}$–like proteins.

The key biochemical difference between rod-like $G\alpha_{t1}'$ and its cone counterpart $G\alpha_{t2}'$ was found to be markedly higher intrinsic nucleotide exchange of $G\alpha_{t2}'$. The region primarily responsible for the increased nucleotide exchange was mapped to residues $G\alpha_{t2}$ (121–219). Gα-subunits of heterotrimeric G proteins are composed of two domains, a GTPase (Ras-like) domain and a helical domain. GDP (or GTP) is buried between the two domains (26, 27). A network of interactions between the two domains is involved in control of basal

nucleotide exchange. Mutations disrupting the interdomain interactions increased the basal nucleotide exchange in $G\alpha_i$ (28). Within $G\alpha_{t2}$ (121–219), a conserved cone-specific residue Ala144 corresponds to the conserved rod-specific Ser140. Ser140 from the helical domain interacts with Asp227 and Lys273 from the Ras-like domain (26, 27). The model of the Ser→Ala substitution using the structure of $G\alpha_t$GDP (27) demonstrates that the interdomain interactions involving Ser140 are disrupted (Fig. 7). Previous study found no evidence for the role of Ser140 in controlling $G\alpha_{t1}$ nucleotide exchange (29). However, a trypsin-protection assay as readout of $G\alpha_{t1}$ activation is severely limited in terms of the kinetic resolution. Our results suggest that the Ser→Ala substitution in $G\alpha_{t2}$ contributes to its high intrinsic nucleotide rate. The $G\alpha_{t1}$′Ser140Ala mutation increased, whereas the $G\alpha_{t2}$′Ala144Ser mutation decreased the nucleotide exchange rates of the respective Gα subunits. The effects of these mutations on the basal GTPγS binding rates were moderate, suggesting the involvement of other residues. $G\beta_1\gamma_1$ did not inhibit the high nucleotide exchange rate of $G\alpha_{t2}$. This agrees with the impairment of the interdomain contacts in $G\alpha_{t2}$ as the cause of its high nucleotide exchange rate. Gβ binds only to the N-terminus and the Ras-like domain of Gα, and, thus may not influence the interdomain interface (12). The finding that the GTPγS-bound $G\alpha_{t2}$ can be isolated through the spontaneous nucleotide exchange supports the notion that native $G\alpha_{t2}$ also has high intrinsic nucleotide exchange rate (9). The functional significance of this phenomenon, if any, remains to be determined. Spontaneous activation of G_{t2} in cones may elevate basal activity of PDE6, potentially altering the sensitivity and kinetics of cone light responses (30).

Our experiments revealed no significant differences in the binding of $G\beta_1\gamma_1$ to $G\alpha_{t1}$′ and $G\alpha_{t2}$′ (Fig. 4), nor in the efficiency of $G\alpha_{t1}$′ and $G\alpha_{t2}$′ activation by R* in the presence of $G\beta_1\gamma_1$ (Fig. 5). However, the rates of activation of non-N-acylated recombinant Gα in the R*, $G\beta_1\gamma_1$-reconstituted system observed previously and in this study are well below the rates of activation of native Gt under similar conditions (13, 31, 32). Thus, our activation paradigm may not be capable of detecting small differences in the R*-Gt coupling for native $G\alpha_{t2}$ and $G\alpha_{t1}$. Moreover, the potential role of cone-specific $G\beta_3\gamma_8$ to transducin/R* coupling has not been investigated in this study. The interdomain interactions in Gα-subunits appear to be essential to receptor-mediated activation of G proteins. Mutant $G\alpha_s$-subunits with disrupted interdomain interactions showed decreased ability for activation by the β-adrenergic receptor (33). The relatively weak interdomain interface in $G\alpha_{t2}$ may potentially reduce the $G\alpha_{t2}$ coupling to R*. Our results seem to favor the idea that the lower amplification in *GNAT2C* rods is linked to the lower efficiency of $G\alpha_{t2}$ coupling to rod PDE6 rather than to R*. Yet, the potency of rod PDE6 activation by $G\alpha_{t2}$GTPγS in solution is not significantly lower than the activation by $G\alpha_{t1}$GTPγS (9). Nonetheless, rod PDE6 activation by $G\alpha_{t1}$ on the membrane is markedly more potent than in solution (34). Alternatively, small reductions in both couplings, R*/$G\alpha_{t2}$ and $G\alpha_{t2}$/PDE6, may result in the combined 2-fold lower amplification in *GNAT2C* rods. In cones, however, a short lifetime of photoactivated cone pigments due to rapid spontaneous decay and pigment phosphorylation, and a lower rate of Gt_2 activation, may dictate the activation phase of photoresponses (8, 35, 36).

The intrinsic GTPase activities of $G\alpha_{t2}$′ and $G\alpha_{t1}$′ were found to be similar. The k_{cat} for the unstimulated GTP hydrolysis by $G\alpha_{t1}$′ is equivalent to the previously reported k_{cat} values of native $G\alpha_{t1}$ (14, 37). Furthermore, the intrinsic GTPase activities of $G\alpha_{t1}$ and $G\alpha_{i1}$ are comparable (14). Thus, the chimeric $G\alpha_t$-subunits appear to faithfully reflect intrinsic GTPase activities of $G\alpha_{t2}$ and $G\alpha_{t1}$, which, in all probability, are similar. The GTPase activity of transducins *in vivo* is far greater than its intrinsic activity owing to the GAP activity of the membrane-bound RGS9 protein complex with the cooperative input from the effector PDE6 (38, 39). The faster rate of transducin inactivation in cones compared to rods may result from the greater potency or the higher expression levels of the RGS9 complex

(14, 40). The former possibility is suggested by the finding that RGS9 is a much more potent GAP for $G\alpha_{t1}$ compared to $G\alpha_{i1}$, and the selectivity determinants reside in the $G\alpha_{t1}$ helical domain (14). Nonetheless, the lack of the difference in the effects of the RGS9d on the GTPase activities of $G\alpha_{t2}$ and $G\alpha_{t1}$ indicates that the efficacies of RGS9 towards cone and rod transducins are not grossly different. This result is consistent with the strong conservation of RGS9-contact residues of transducin (41) and supportive of RGS9 protein levels as a determining factor in transducin inactivation. The rate of transducin inactivation is regulated by the membrane attachment of the RGS9 GAP complex (42, 43). Therefore, further studies with the use of the N-acylated $G\alpha_t$ subunits are needed to probe the selectivity of the RGS9 GAP complex.

Supplementary Material

Refer to Web version on PubMed Central for supplementary material.

Abbreviations

$G\alpha_{t1}$	rod transducin α-subunit
$G\alpha_{t2}$	cone transducin α-subunit
$G\alpha_{t2}'$	$G\alpha_{t2}/G\alpha_{i1}$ chimera
PDE6	photoreceptor phosphodiesterase-6
R*	photoexcited rhodopsin
RGS9	regulator of G-protein signaling 9
GTPγS	guanosine 5′-O-(3-thiotriphosphate)

References

1. Burns ME, Arshavsky VY. Beyond counting photons: trials and trends in vertebrate visual transduction. Neuron. 2005; 48:387–401. [PubMed: 16269358]
2. Lamb TD, Pugh EN Jr. Phototransduction, dark adaptation, and rhodopsin regeneration the proctor lecture. Invest Ophthalmol Vis Sci. 2006; 47:5137–5152. [PubMed: 17122096]
3. Fu Y, Yau KW. Phototransduction in mouse rods and cones. Pflugers Archiv. 2007; 454:805–819. [PubMed: 17226052]
4. Nikonov SS, Kholodenko R, Lem J, Pugh EN Jr. Physiological features of the S- and M-cone photoreceptors of wild-type mice from single-cell recordings. J Gen Physiol. 2006; 127:359–374. [PubMed: 16567464]
5. Kefalov V, Fu Y, Marsh-Armstrong N, Yau K. Role of visual pigment properties in rod and cone phototransduction. Nature. 2003; 425:526–531. [PubMed: 14523449]
6. Deng WT, Sakurai K, Liu J, Dinculescu A, Li J, Pang J, Min SH, Chiodo VA, Boye SL, Chang B, Kefalov VJ, Hauswirth WW. Functional interchangeability of rod and cone transducin *α*-subunits. Proc Natl Acad Sci U S A. 2009; 106:17681–17686. [PubMed: 19815523]
7. Chen CK, Woodruff ML, Chen FS, Shim H, Cilluffo MC, Fain GL. Replacing the rod with the cone transducin subunit decreases sensitivity and accelerates response decay. J Physiol. 2010; 588:3231–3241. [PubMed: 20603337]
8. Tachibanaki S, Shimauchi-Matsukawa Y, Arinobu D, Kawamura S. Molecular mechanisms characterizing cone photoresponses. Photochem Photobiol. 2007; 83:19–26. [PubMed: 16706600]
9. Muradov H, Boyd KK, Artemyev NO. Rod phosphodiesterase-6 PDE6A and PDE6B subunits are enzymatically equivalent. J Biol Chem. 2010; 285:39828–39834. [PubMed: 20940301]
10. Pugh EN Jr, Lamb TD. Amplification and kinetics of the activation steps in phototransduction. Biochim Biophys Acta. 1993; 1141:111–1149. [PubMed: 8382952]

11. Krispel CM, Chen D, Melling N, Chen Y, Martemyanov KA, Quillinan N, Arshavsky VY, Wensel TG, Chen C, Burns ME. RGS expression rate-limits recovery of rod photoresponses. Neuron. 2006; 51:409–416. [PubMed: 16908407]
12. Lambright DG, Sondek J, Bohm A, Skiba NP, Hamm HE, Sigler PB. The 2.0 Å crystal structure of a heterotrimeric G protein. Nature. 1996; 379:311–319. [PubMed: 8552184]
13. Skiba NP, Bae H, Hamm HE. Mapping the effector binding sites of transducin α-subunit using Gαt/Gαi1 chimeras. J Biol Chem. 1996; 271:413–424. [PubMed: 8550597]
14. Skiba NP, Yang CS, Huang T, Bae H, Hamm HE. The α-helical domain of Gαt determines specific interaction with regulator of G protein signaling 9. J Biol Chem. 1999; 274:8770–8778. [PubMed: 10085118]
15. Papermaster DS, Dreyer WJ. Rhodopsin content in the outer segment membranes of bovine and frog retinal rods. Biochemistry. 1974; 13:2438–2444. [PubMed: 4545509]
16. Yamanaka G, Eckstein F, Stryer L. Stereochemistry of the guanyl nucleotide binding site of transducin probed by phosphorothionate analogues of GTP and GDP. Biochemistry. 1985; 24:8094–8101. [PubMed: 3004574]
17. Ford CE, Skiba NP, Bae H, Daaka Y, Reuveny E, Shekter LR, Rosal R, Weng G, Yang CS, Iyengar R, Miller RJ, Jan LY, Lefkowitz RJ, Hamm HE. Molecular basis forinteractions of G protein βγ subunits with effectors. Science. 1998; 280:1271–1274. [PubMed: 9596582]
18. Natochin M, Artemyev NO. A point mutation uncouples transducin-α from the photoreceptor RGS and effector proteins. J Neurochem. 2003; 87:1262–1271. [PubMed: 14622106]
19. Arshavsky VY, Gray-Keller MP, Bownds MD. cGMP suppresses GTPase activity of a portion of transducin equimolar to phosphodiesterase in frog rod outer segments. J Biol Chem. 1991; 266:18530–18537. [PubMed: 1655754]
20. Linder ME, Pang IH, Duronio RJ, Gordon JI, Sternweis PC, Gilman AG. Lipid modifications of G protein subunits. Myristoylation of Goα increases its affinity for βγ. J Biol Chem. 1991; 266:4654–4659. [PubMed: 1900297]
21. Natochin M, Muradov KG, McEntaffer RL, Artemyev NO. Rhodopsin recognition by mutant Gsα containing C-terminal residues of transducin. J Biol Chem. 2000; 275:2669–2675. [PubMed: 10644728]
22. van Dop C, Yamanaka G, Steinberg F, Sekura RD, Manclark CR, Stryer L, Bourne HR. ADP-ribosylation of transducin by pertussis toxin blocks the light-stimulated hydrolysis of GTP and cGMP in retinal photoreceptors. J Biol Chem. 1984; 259:23–26. [PubMed: 6142883]
23. Watkins PA, Burns DL, Kanaho Y, Liu TY, Hewlett EL, Moss J. ADP-ribosylation of transducin by pertussis toxin. J Biol Chem. 1985; 260:13478–13482. [PubMed: 3863817]
24. West RE Jr, Moss J, Vaughan M, Liu T, Liu TY. Pertussis toxin-catalyzed ADP-ribosylation of transducin. Cysteine 347 is the ADP-ribose acceptor site. J Biol Chem. 1985; 260:14428–14430. [PubMed: 3863818]
25. Zhang X, Wensel TG, Yuan C. Tokay gecko photoreceptors achieve rod-like physiology with cone-like proteins. Photochem Photobiol. 2006; 82:1452–1460. [PubMed: 16553462]
26. Noel JP, Hamm HE, Sigler PB. The 2.2A crystal structure of transducin-α complexed with GTPγS. Nature. 1993; 366:654–663. [PubMed: 8259210]
27. Lambright DG, Noel JP, Hamm HE, Sigler PB. Structural determinants for activation of the α-subunit of a heterotrimeric G protein. Nature. 1994; 369:621–628. [PubMed: 8208289]
28. Remmers AE, Engel C, Liu M, Neubig RR. Interdomain interactions regulate GDP release from heterotrimeric G proteins. Biochemistry. 1999; 38:13795–13800. [PubMed: 10529224]
29. Marin EP, Krishna AG, Archambault V, Simuni E, Fu WY, Sakmar TP. The function of interdomain interactions in controlling nucleotide exchange rates in transducin. J Biol Chem. 2001; 276:23873–23880. [PubMed: 11290746]
30. Nikonov S, Lamb TD, Pugh EN Jr. The role of steady phosphodiesterase activity in the kinetics and sensitivity of the light-adapted salamander rod photoresponse. J Gen Physiol. 2001; 116:795–824. [PubMed: 11099349]
31. Barren B, Natochin M, Artemyev NO. Mutation R238/E in transducin-α yields a GTPase and effector-deficient, but not dominant-negative G-protein α-subunit. Mol Vis. 2006; 12:492–498. [PubMed: 16735989]

32. Gopalakrishna KN, Doddapuneni K, Boyd KK, Masuho I, Martemyanov KA, Artemyev NO. Interaction of transducin with uncoordinated 119 protein (UNC119): implications for the model of transducin trafficking in rod photoreceptors. J Biol Chem. 2011; 286:28954–28962. [PubMed: 21712387]
33. Grishina G, Berlot CH. Mutations at the domain interface of Gsα impair receptor-mediated activation by altering receptor and guanine nucleotide binding. J Biol Chem. 1998; 273:15053–15060. [PubMed: 9614114]
34. Malinski JA, Wensel TG. Membrane stimulation of cGMP phosphodiesterase activation by transducin: comparison of phospholipid bilayers to rod outer segment membranes. Biochemistry. 1992; 31:9502–9512. [PubMed: 1327116]
35. Imai H, Kojima D, Oura T, Tachibanaki S, Terakita A, Shichida Y. Single amino acid residue as a functional determinant of rod and cone visual pigments. Proc Natl Acad Sci USA. 1997; 94:2322–2326. [PubMed: 9122193]
36. Kennedy MJ, Dunn FA, Hurley JB. Visual pigment phosphorylation but not transducin translocation can contribute to light adaptation in zebrafish cones. Neuron. 2004; 41:915–928. [PubMed: 15046724]
37. Natochin M, Granovsky AE, Artemyev NO. Regulation of transducin GTPase activity by human retinal RGS. J Biol Chem. 1997; 272:17444–17449. [PubMed: 9211888]
38. He W, Cowan CW, Wensel TG. RGS9, a GTPase accelerator for phototransduction. Neuron. 1998; 20:95–102. [PubMed: 9459445]
39. Skiba NP, Hopp JA, Arshavsky VY. The effector enzyme regulates the duration of G protein signaling in vertebrate photoreceptors by increasing the affinity between transducin and RGS protein. J Biol Chem. 2000; 275:32716–32720. [PubMed: 10973941]
40. Zhang X, Wensel TG, Kraft TW. GTPase regulators and photoresponses in cones of the eastern chipmunk. J Neurosci. 2003; 23:1287–1297. [PubMed: 12598617]
41. Slep KC, Kercher MA, He W, Cowan CW, Wensel TG, Sigler PB. Structural determinants for regulation of phosphodiesterase by a G protein at 2.0 A. Nature. 2001; 409:1071–1077. [PubMed: 11234020]
42. Hu G, Wensel TG. R9AP, a membrane anchor for the photoreceptor GTPase accelerating protein, RGS9-1. Proc Natl Acad Sci USA. 2002; 99:9755–9760. [PubMed: 12119397]
43. Lishko PV, Martemyanov KA, Hopp JA, Arshavsky VY. Specific binding of RGS9-Gβ5L to protein anchor in photoreceptor membranes greatly enhances its catalytic activity. J Biol Chem. 2002; 277:24376–24381. [PubMed: 12006596]
44. Guex N, Peitsch MC. SWISS-MODEL and the Swiss-PdbViewer: an environment for comparative protein modeling. Electrophoresis. 1997; 18:2714–2723. [PubMed: 9504803]
45. DeLano, WL. The PyMOL molecular graphics system. 2004. http://www.pymol.org

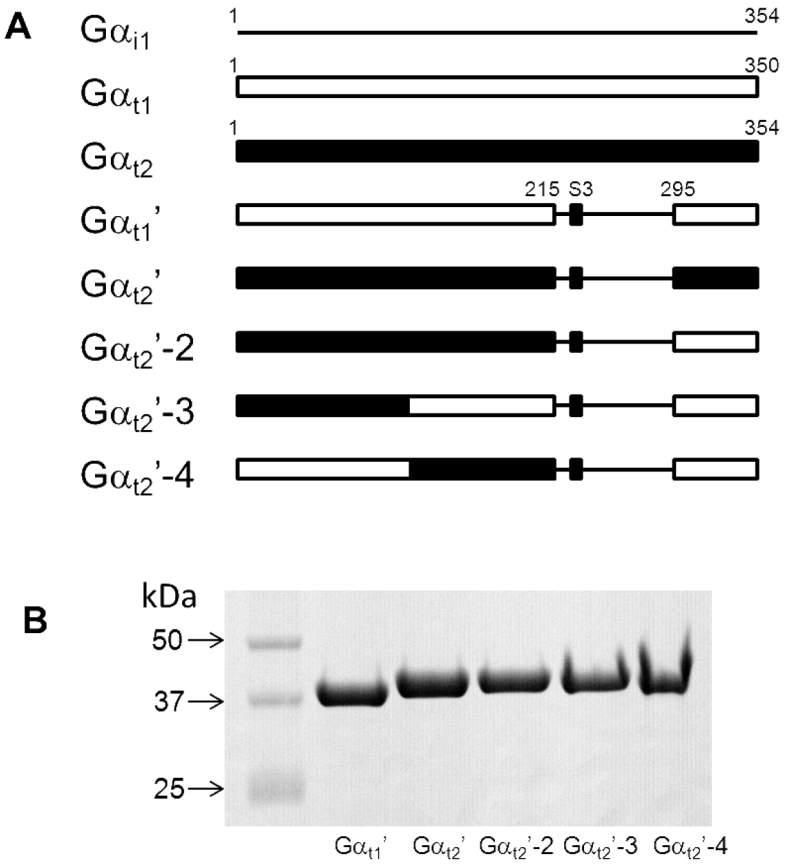

Figure 1.

(**A)**. Schematic representation of $G\alpha_t$ chimeras. The switch III region (S3, $G\alpha_{t1}$-228-236) (black) is identical in $G\alpha_{t1}$ and $G\alpha_{t2}$. (**B)**. Coomassie blue-stained SDS-gel showing purified $G\alpha_t$ chimeras. Samples represent equal fractions of the preparations from 0.5 liter bacterial cultures.

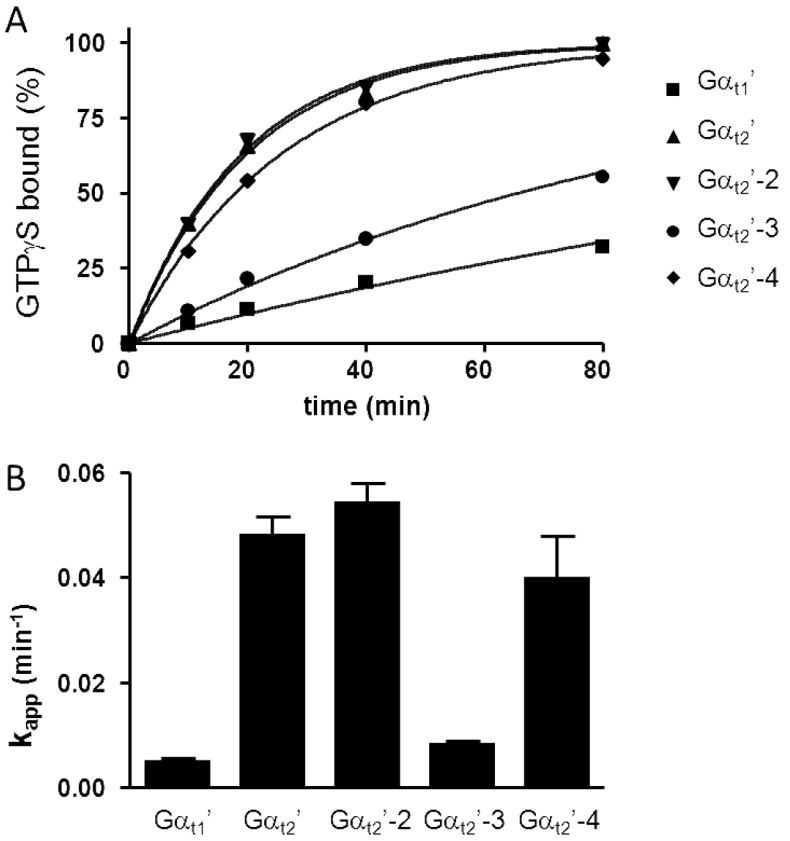

Figure 2.

(A). Spontaneous GTPγS binding to $G\alpha_{t1}'$ and $G\alpha_{t2}'$-chimeras. The binding of GTPγS to $G\alpha_{t1}'$ and $G\alpha_{t2}'$-chimeras (1 μM each) was initiated with the addition of 5 μM [^{35}S]GTPγS. Gα-bound GTPγS was counted by withdrawing aliquots at the indicated times and passing them through Whatman cellulose nitrate filters. Results from one of four similar experiments are shown. **(B)** k_{app} values (min^{-1}) (mean±SE) of intrinsic GTPγS binding to chimeric $G\alpha_t$-proteins were calculated from four experiments such as shown in **A**.

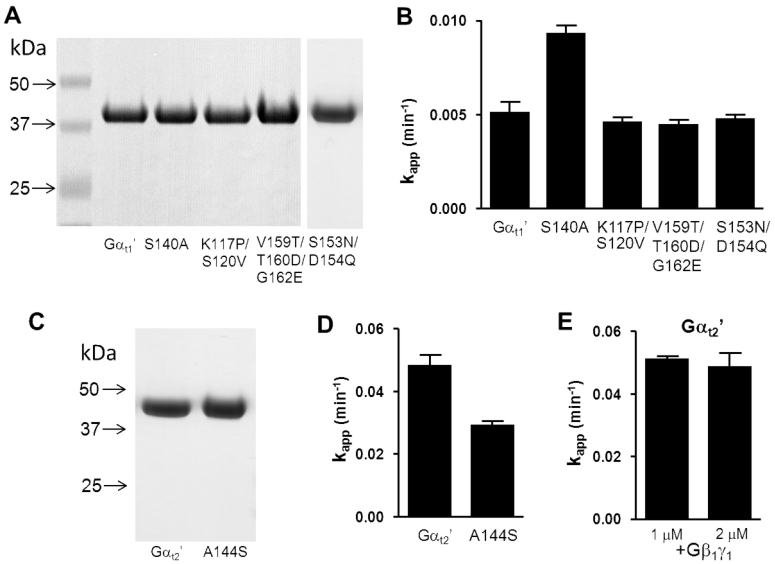

Figure 3.

(A, C) Coomassie blue-stained SDS-gel showing purified mutant $G\alpha_{t1}'$- and $G\alpha_{t2}'$-subunits. Samples represent equal fractions of the preparations from 0.5 liter bacterial cultures. **(B, D)** k_{app} values (min^{-1}) (mean±SE) of intrinsic GTPγS binding to mutant $G\alpha_{t1}'$ and $G\alpha_{t2}'$ calculated from four binding experiments for each mutant. (**E**). k_{app} values (min^{-1}) (mean ±SE) of intrinsic GTPγS binding to mutant $G\alpha_{t2}'$ (1 μM) in the presence of 1 and 2 μM $G\beta_1\gamma_1$.

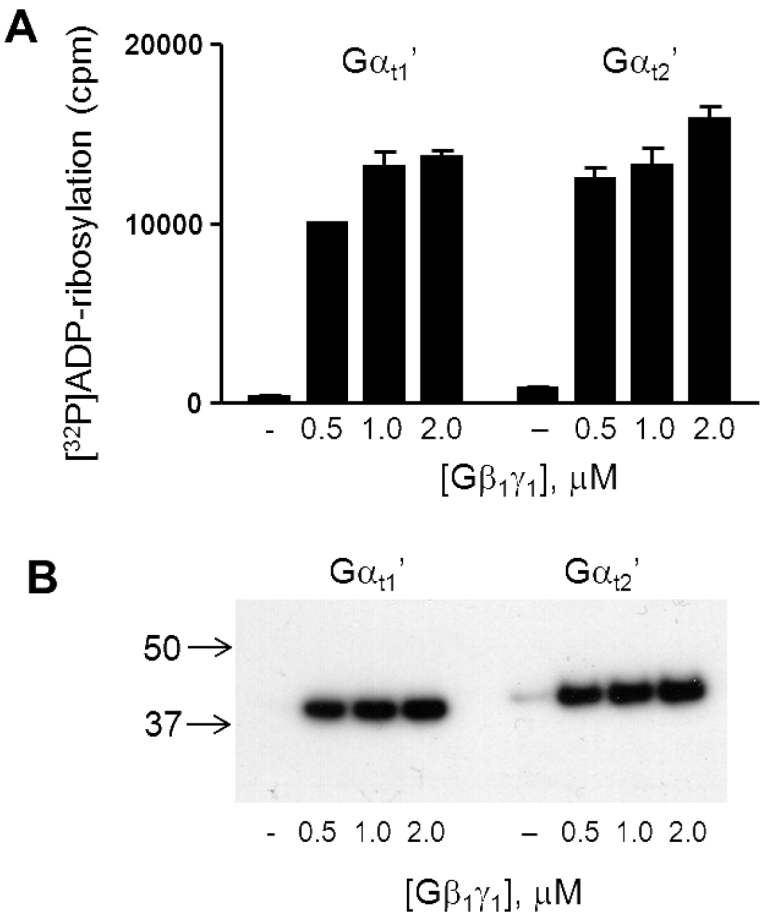

Figure 4. The $G\beta_1\gamma_1$-dependent ADP-ribosylation of $G\alpha_{t1}'$ and $G\alpha_{t2}'$

Pertussis toxin-catalyzed ADP-ribosylation of $G\alpha_{t1}'$ and $G\alpha_{t2}'$ (0.5 μM each) was carried out in the presence of increasing concentrations of $G\beta_1\gamma_1$. (**A**) [32P]ADP-ribosylation of $G\alpha_{t1}'$ and $G\alpha_{t2}'$ is analyzed by liquid scintillation counting (mean±SE, n=3). (**B**) Aliquots from the ADP-ribosylation reaction mixtures were analyzed by SDS-PAGE followed by autoradiography.

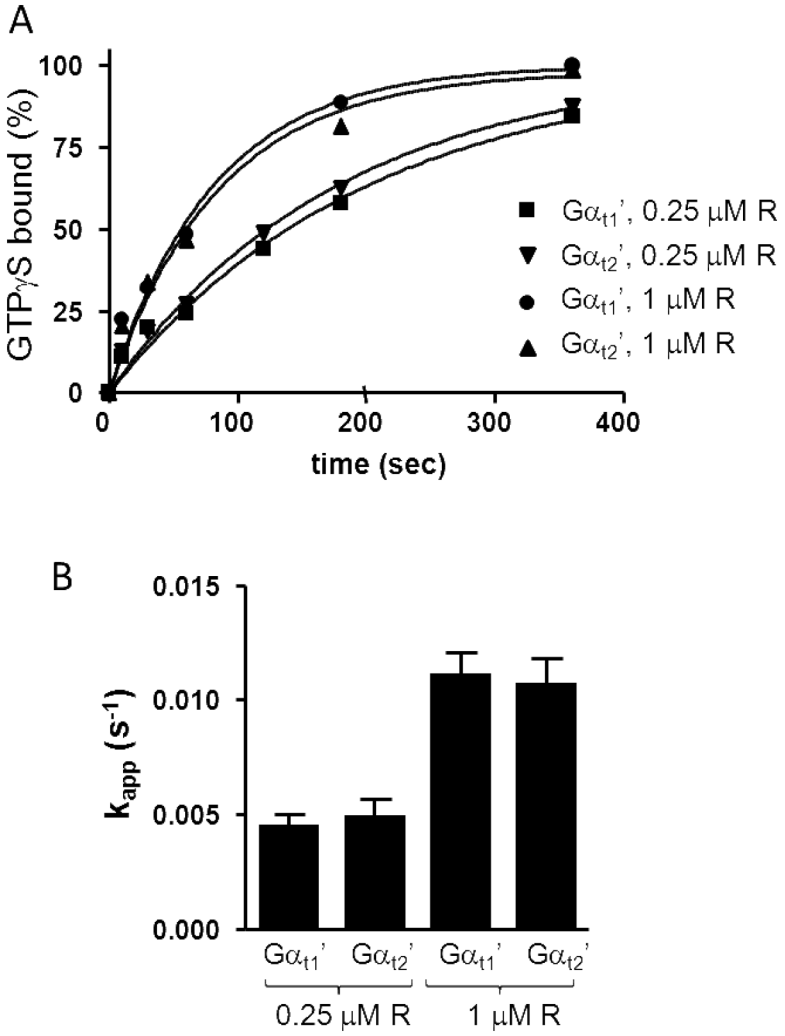

Figure 5.

(A) Rhodopsin-catalyzed GTPγS binding to $G\alpha_{t1}'$ and $G\alpha_{t2}'$. The binding of GTPγS to $G\alpha_{t1}'$ and $G\alpha_{t2}'$ (1 μM each) in the presence of 1 μM $G\beta_1\gamma_1$ and uROS membranes (0.25 or 1 μM rhodopsin) was initiated with the addition of 5 μM [^{35}S]GTPγS. Gα-bound GTPγS was counted by withdrawing aliquots at the indicated times and passing them through Whatman cellulose nitrate filters. Results from one of four similar experiments are shown. **(B)** k_{app} values (s^{-1}) (mean±SE) of intrinsic GTPγS binding to chimeric $G\alpha_t$-proteins were calculated from four experiments such as shown in **A.**

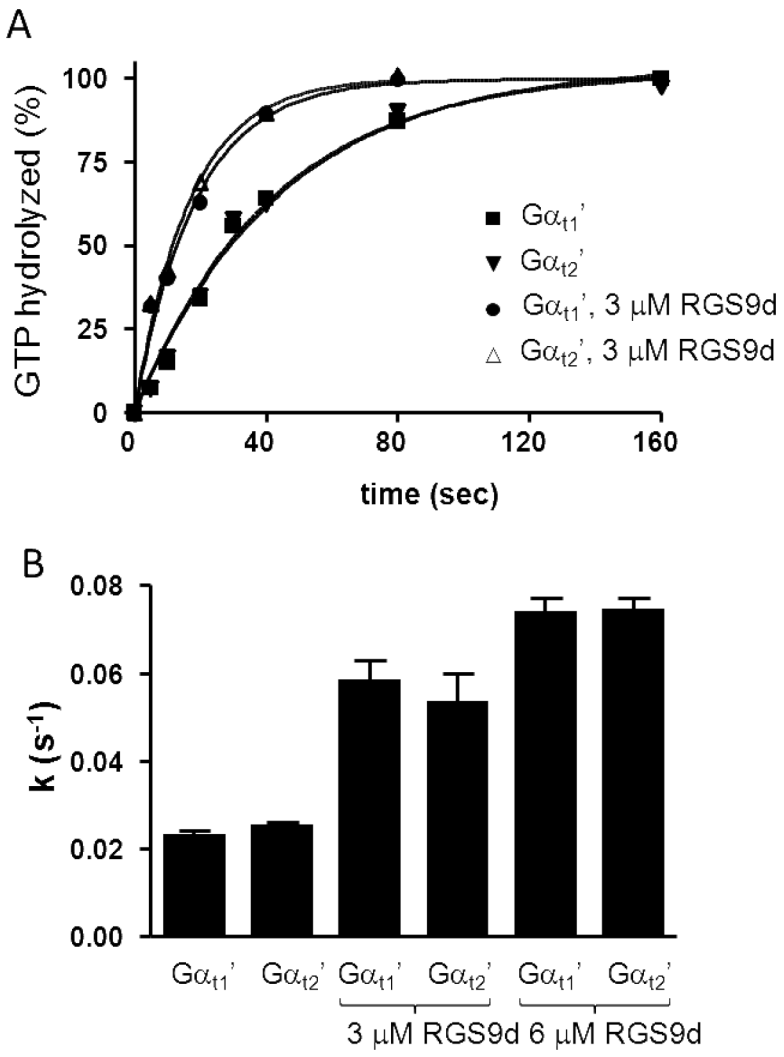

Figure 6. Single turnover GTPase assays of $G\alpha_{t1}'$ and $G\alpha_{t2}'$. Effects of RGS9d

(A) Single-turnover GTPase activity measurements were carried out in suspensions of uROS membranes (10 μM rhodopsin) reconstituted with chimeric $G\alpha_t$ subunits (1 μM) and $G\beta_1\gamma_1$ (1 μM). Where indicated, RGS9d was added. Reactions were started with the addition of 100 nM [γ-^{32}P]GTP and free $^{32}P_i$ was measured by liquid scintillation. Results from one of three similar experiments are shown. (**B**) The k_{cat} values (s^{-1}) (mean±SE) for GTP hydrolysis by chimeric $G\alpha_t$-proteins were calculated from three experiments such as shown in **A.**

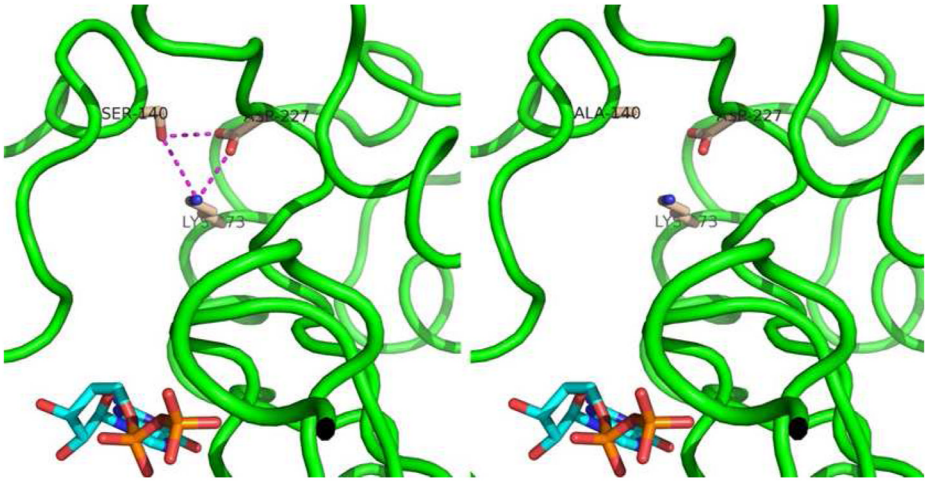

Figure 7. Interdomain interactions of Ser140 in rod $G\alpha_{t1}$ are lost in the S140A mutant

In the structure of $G\alpha_{t1}$GDP (24), $G\alpha_{t1}$Ser140 from the helical domain interacts with Asp227 and Lys273 from the Ras-like domain (*left*). The S140A mutation was introduced into the structure of $G\alpha_{t1}$GDP using the Swiss-PdbViewer (v.4) (44). The mutation disrupts the interdomain interactions in $G\alpha_{t1}$GDP (*right*). The images were produced using PyMOL 1.4.1 (45).